

Parametric Carrier Sizing for Pressurized Rover Resupply Operations

Nathnael F. Geneti*, Bradford Robertson†, Dimitri Mavris‡
Georgia Institute of Technology, Atlanta, GA, 30332

The Artemis program aims to establish a lunar base near the south pole of the Moon, with plans that potentially include a surface habitat and other surface elements, such as a pressurized rover. To ensure continuous operation, these elements require regular cargo resupply that includes consumables necessary for mission success that are not installed as part of the vehicle. Resupply cargo will be delivered via specialized logistic carrier modules, whose design can benefit greatly from understanding the impact of high-level design alternatives. This study introduces a parametric framework for sizing logistic carrier modules, with emphasis on the impact of these high-level design choices. The framework outlines structural sizing requirements to accommodate resupply consumables, along with the thermal and power subsystems needed to maintain temperature stability and supply power during independent carrier operation. Trade-offs between larger, integrated carriers, capable of resupplying both the habitat and a pressurized rover, and smaller specialized carriers for pressurized rover resupply are evaluated. The framework's capabilities are then demonstrated through sensitivity analysis and design space exploration for a use case mission.

I. Nomenclature

R	=	carrier internal radius
h_{int}	=	internal walkway height
w_{int}	=	internal walkway width
V	=	carrier internal volume
A_{cs}	=	cross-sectional area
L	=	walkway length
L_{PV}	=	pressure vessel length
t_{min_H}	=	minimum thickness - hoop stress
t_{min_L}	=	minimum thickness - longitudinal stress
SA_{PV}	=	pressure vessel surface area
m_{PV}	=	pressure vessel mass
ρ_{Al}	=	density of aluminum
m_{rack}	=	consumable storage rack mass
m_{sbeam}	=	arc beam and saddle structure mass
m_{rad}	=	radiator mass
m_{bat}	=	battery mass
m_{carrier}	=	total carrier mass
V_{carrier}	=	total carrier volume
SF	=	safety factor
$pack_{\text{Eff}}$	=	Packing Efficiency

*Graduate Research Associate, Aerospace Systems Design Laboratory, School of Aerospace Engineering, AIAA Student Member.

†Senior Research Engineer and Chief of Space Systems & Technologies Division of ASDL, Aerospace Systems Design Laboratory, School of Aerospace Engineering, Senior AIAA Member.

‡Georgia Tech Distinguished Regents Professor and Director of ASDL, Aerospace Systems Design Laboratory, School of Aerospace Engineering, AIAA Fellow.

II. Introduction

NASA's current Moon to Mars architecture aims to establish a lunar base near the south pole of the Moon to demonstrate technical and economic feasibility before extending exploration to Mars and beyond. This objective is to be achieved through four successive mission segments with progressively increasing complexity. The first segment involves returning humans to the Moon, while the second segment, termed the Foundational Exploration segment, enhances lunar missions by expanding operations and capabilities, increasing mission durations and mobility, and preparing for future Mars missions through advanced exploration and infrastructure development. Subsequent segments will aim to build economic opportunities, enable broader participation in lunar science and exploration, and ultimately establish a human presence on Mars [1].

As part of the Foundational Exploration segment, dedicated surface habitation and mobile surface habitation via pressurized rovers are crucial for maintaining a continuous presence on the lunar surface. These elements support longer-duration missions, increase crew size, enhance surface utilization, and facilitate extravehicular activity (EVA) explorations [2]. Both habitation and mobility systems will require periodic resupply to ensure crew safety and maintain life support functions throughout their operational life cycles. Resupply logistics encompass all required equipment and supplies, excluding vehicle propellant and pressurants, and are commonly grouped into six categories. Consumables include essential items such as food, clothing, hygiene products, and gases. Maintenance items refer to planned replacements for systems with defined service lives, while spares are intended for unplanned system failures. Utilization items support scientific investigations and technology demonstrations. Outfitting refers to subsystem components delivered after initial deployment for permanent installation. Finally, packaging, overhead, and carrier materials are necessary for the safe transport and storage of logistics items [3].

This study focuses on the consumables, spares, and their packaging needed to resupply a pressurized rover on a regular basis. Estimating the amount of consumables required depends on various mission parameters, such as the number of crew, mission duration, number of EVAs, and the Environmental Control Life Support System (ECLSS) closure [4]. Consumables are categorized into solids, liquids, and gases, and the consumption rate for each category is derived from previous studies [4] and [5]. A tool was developed to approximate the overall mass and volume of these consumables and their packaging for resupplying a pressurized rover across varying mission parameters.

Although no pressurized rover has been used on extraterrestrial bodies to date, resupply missions to the International Space Station (ISS) using the Multi-Purpose Logistics Module (MPLM) provide a relevant model [6]. The MPLM, a pressurized cargo container, transfers supplies and equipment to and from the ISS. Similarly, a logistics carrier is needed to resupply a pressurized rover on the lunar surface. To achieve this, design trades must be conducted to appropriately size the logistics carrier and identify trade-offs between various design parameters, thereby preventing costly errors by understanding the impact of top-level requirements on the final design.

This study presents a parametric framework for evaluating logistics carrier modules designed to support resupply of a pressurized rover on the lunar surface. The logistics module is parameterized to accommodate resupply consumables and their packaging. A parametric tool was developed used to evaluate the impact of high-level parameter changes on the final sizing of the logistics carrier. Sensitivity and constraint analysis were then conducted to examine the variability of key output metrics and explore the feasible design space by comparing various carrier configurations.

This paper is organized into seven sections. The first section presents the nomenclature of key variables. The second section introduces the study. The third section provides background on precedents used as references and an overview of NASA's current resupply architecture. The fourth section outlines the study's methodology, detailing the parametrization of models used in the MDAO framework for conducting trade studies and describing the problem setup for generating surrogate models that enable sensitivity and constraint analysis. The fifth section introduces a case study to demonstrate the developed model's capability and outlines the assumptions used in the study. The sixth section presents the study's results, including an analysis of the use case resupply mission. Finally, the seventh section discusses the study's concluding remarks.

III. Background

A. Precedents

While there are no deployed or fully developed logistics carrier modules for lunar resupply missions, several concepts have been proposed to fulfill similar needs. Two recent NASA studies examined analogous architectures for Mars surface logistics. One study explored a pressurized container system for transporting water extracted via in-situ resource utilization (ISRU), focusing on thermal regulation, power supply, fluid transfer interfaces, and mobility using

a pallet-and-rover system [7]. A follow-up study extended the concept to cryogenic propellant transport, detailing additional complexities such as insulation for LOX and methane, autonomous umbilical mating, leak checking, and pressure management to enable propellant delivery to a Mars Ascent Vehicle [8]. Both studies adopted a pallet-based structure mounted on a rover platform, similar to the chariot mobility system originally proposed in [9]. Trent et al. [10] presented a conceptual transportation architecture for Mars surface missions, proposing a family of modular and reusable cargo and crew vehicles including landers, tankers, and mobile assets, designed to support large scale ISRU and surface operations with efficient mass delivery and reuse strategies. Another study from 1992 discussed the design of a complete pressurized rover [11]. This study detailed the design of cylindrical hulls to provide a safe and functional pressurized environment for crew and equipment. Similar to the previous study, this design also presented a point design of a cylindrical pressurized container as part of a pressurized rover, incorporating thermal and power systems along with other subsystems to meet the thermal control, power, and movement requirements of the rover.

Building on this study, the Aerospace Systems Design Laboratory of Georgia Institute of Technology developed a parametric framework for sizing a lunar pressurized rover to evaluate how changes in high-level requirements affect the final rover design. Cardenas et al. [12] discussed the structural modeling of the framework, and Harding et al. [13] outlined the power and thermal modeling of the framework.

B. Lunar Resupply Architecture Overview

NASA’s current notional architecture for a sustained lunar presence at the lunar south pole includes core elements such as the Surface Habitat (SH), Pressurized Rover (PR), Lunar Terrain Vehicle (LTV), power systems, and ISRU systems. The SH serves as the main habitation module of the base camp, accommodating up to four crew members for 30 days, with the potential to evolve to support up to 60 days in the long term. The PR functions as a mobile habitation module, enabling extended trips away from the base camp. During the approximately 30-day mission, it is assumed that the crew of four will split into two groups, with two residing in the PR. The groups will then swap mid-mission, after 15 days [14]. It is important to note that these concepts of operations (ConOps) are notional and subject to change as more design trades are conducted.

Cargo delivery to the lunar surface can be accomplished using various cargo landers with different payload capabilities. According to the spring 2024 Lunar Surface Innovation Consortium (LSIC) meeting summary report [15], cargo can be delivered using several lander options including Commercial Lunar Payload Service (CLPS) landers (up to 400 kg), Blue Moon MK1 lander (up to 3000 kg), MK2 lander (up to 20,000 kg), and the largest lander, SpaceX’s Starship Cargo lander (up to 100,000 kg), as shown in Fig. 1.

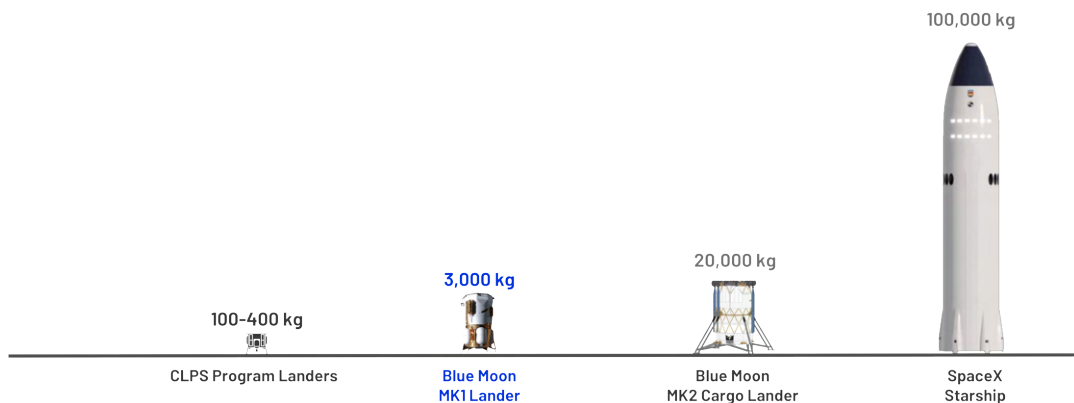


Fig. 1 Lunar Cargo Landers [15]

NASA’s Moon to Mars 2024 architecture concept review white paper on Lunar Surface Cargo [16] forecasts a cargo demand for resupply missions in the range of 2,500 kg to 10,000 kg per year in the foundational exploration segment of the architecture. The paper notes a gap in lander capability for this class of cargo resupply missions, as CLPS landers are too small, and human-class delivery landers are too large for recurring missions.

Incoming cargo is enclosed in a pressurized module similar to the Multi-Purpose Logistics Module (MPLM) used with the ISS. This module could be deployed in one of two configurations: a single large carrier containing resupply cargo for both the SH and PR, or separate specialized modules that resupply the SH and PR separately, as shown in Fig.

2 and Fig.3 respectively. The graphic CAD models are notional representations to explain the concept and do not reflect the final designs of future missions.

Large logistics carriers reduce overall system complexity by enabling simultaneous resupply of both the SH and the PR. However, this requires crew members to transfer resupply cargo from the SH to the PR. It is typically assumed that a pressurized tunnel connects the SH and PR, as described in [17], allowing astronauts to move between the SH and PR without extravehicular activities (EVAs). Conversely, smaller specialized carriers reduce manual work for crew members by docking directly to the PR, providing more time for scientific operations.

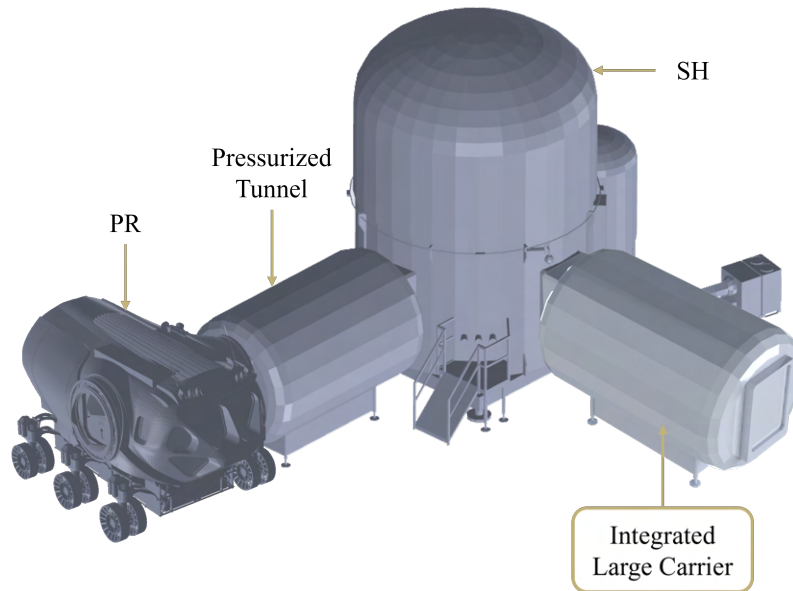


Fig. 2 Large Carrier Resupply Operation (The PR & SH CAD parts are sourced from NASA’s publicly available CAD models)

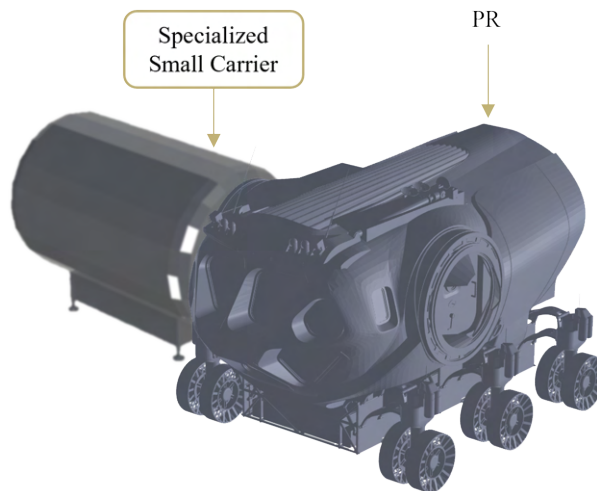


Fig. 3 Small Carrier Resupply Operation (The PR CAD model is sourced from NASA’s publicly available CAD models)

IV. Methodology

The overall methodology to set up the parametric framework for sizing a logistics carrier using a predefined set of high-level input parameters in this study is summarized in Fig.4.



Fig. 4 Study Outline

A. Defining High-level Inputs

High-level inputs are mission parameters that define a class of carrier point designs. These parameters dictate the consumption rate of the resupply consumables, which in turn influences the overall mass and volume of these consumables and their packaging, ultimately determining the sizing of the carrier. These parameters include the number of crew, mission duration, ECLSS closure, and the number of EVAs. Variations in these input parameters represent different mission scenarios, which in turn determine the appropriate size for the logistics carrier. The input combinations utilized in this study are detailed in Table 1, covering a total of 160 mission scenarios.

Table 1 Mission Parameter Inputs

Variables	Alternatives
Number of Crew	2, 4
Mission Duration	7, 14, 21, 28
ECLSS Type (Closure)	Open, Closed
Number of EVAs	1, 2, 3, ... 10

B. Logistic Resupply Approximation Tool

For a given set of mission parameters, the mass and volume of each consumable needed to resupply a pressurized rover is computed using the consumption and packaging rates provided by [4] and [5]. These consumption rates are informed by historical resupply usage data from the International Space Station (ISS), the Baseline Values and Assumptions Document (BVAD) [18], and the Human Integration Design Handbook [19], among other sources.

Resupply consumables are categorized into solids, liquids, and gases based on their packaging. Solid consumables include items such as food, healthcare supplies, hygiene kits, and operational supplies, which are packaged in Cargo Transfer Bags (CTBs). The primary liquid consumable for this study is water, used for drinking, food re-hydration, and Waste Collection and Storage (WCS) flushes. Liquid consumables are stored in Contingency Water Containers – Iodine (CWC-I) and delivered in M02 bags, with each M02 bag capable of holding up to three CWC-Is. The gaseous consumables considered include oxygen and nitrogen, with high-pressure oxygen for EVA delivered separately from low-pressure oxygen needed for metabolic and other purposes. All gaseous consumables are stored in High Pressure Gas Containers (HPGC) and delivered in M01 bags. The maximum amount of consumable packed is determined either by the mass or geometric constraint of their packaging, whichever is reached first. However, the geometric constraint is typically reached first and usually dictates the amount of consumable packed per the respective packaging. Table 2 shows the mass and volume constraints used in the packaging of consumables.

The level of ECLSS closure (degree of recycling) is another key parameter to be accounted for. Akin et al. [20] assume an open ECLSS where the PR relies on the lunar base for all recycling operations, thus requiring continuous resupply of consumables. Burke et al. [21] state that even the SH currently depends on the resupply of goods and water through small logistics carriers. While an open-loop ECLSS has lower cost and risk to habitation, a closed-loop system significantly decreases the logistics resupply mass, as will be shown in the results section of this study. Consequently, research is being conducted towards developing a closed ECLSS for a pressurized rover using the Lunar Electric Rover (LER) prototype [22]. The logistics approximation tool used in this study accounts for both open and closed ECLSS. The closed ECLSS assumes that the pressurized rover can recycle water from crew outputs such as perspiration, respiration, and urine. This recycled water can be used in the Oxygen Generation System (OGS) to produce the necessary

low-pressure oxygen. The hydrogen produced from the OGS can then be combined with a portion of the processed carbon dioxide from metabolic activities using the sabatier process to produce additional water and methane, thereby reducing the amount of liquid and gaseous consumables needed for resupply.

The total mass and volume of the consumables required for resupply is the sum of each consumable for the given mission parameters, plus the mass and volume of the packaging. For fluids (liquids and gases), a small portion (0.5 Kg/tanker) is assumed to be unrecoverable. The respective mass and volume of the packaging used in this study are summarized in Table 3.

Table 3 Packaging Mass and Volume

Item	Value
CWC-I empty mass (Kg)+ ullage	1.22
M02 bag mass (Kg)	8.16
M02 bag volume (m ³)	0.212
Average CTBE mass (Kg)	0.83
CTBE External Vol, raw	0.053
HPGC tank empty mass (Kg)	53.2
M01 bag mass (Kg)	4.83
M01 bag volume (m ³)	0.318

Table 2 Packaging Constraints

Item	Value
CTBE m_limit (Kg)	26.8
CTBE V_limit (m ³)	0.049
CWC-I H ₂ O m_limit (Kg)	21.7
HPGC tank N ₂ m_limit (Kg)	31.2
HPGC tank O ₂ m_limit (Kg)	35.6

C. MDAO Framework

The parametric framework developed in this study was built using NASA’s open-source Multidisciplinary Design Analysis and Optimization (MDAO) framework [23] to perform trade studies on logistics carrier modules for resupplying a pressurized rover. The first step in the development of the MDAO framework to size a logistics carrier module is to define the basic functions of the carrier module. These functions are then organized and connected based on their inter-dependencies, as illustrated in Fig. 5. This figure presents a simplified representation of the N² diagram generated from OpenMDAO. The actual N² generated from OpenMDAO is shown in Appendix A. Each function is a physics-based model from which key output metrics are computed.

The Pressurized Vessel (PV) structure model is based on previous work by Cardenas et al. [12] from ASDL at Georgia Institute of Technology. The Power and Thermal control models are derived from a study by Harding et al. [13], also from ASDL. This paper primarily focuses on the modifications made to the PV Structure model to ensure it is appropriately sized to transport resupply cargo in a pressurized and environmentally controlled manner.

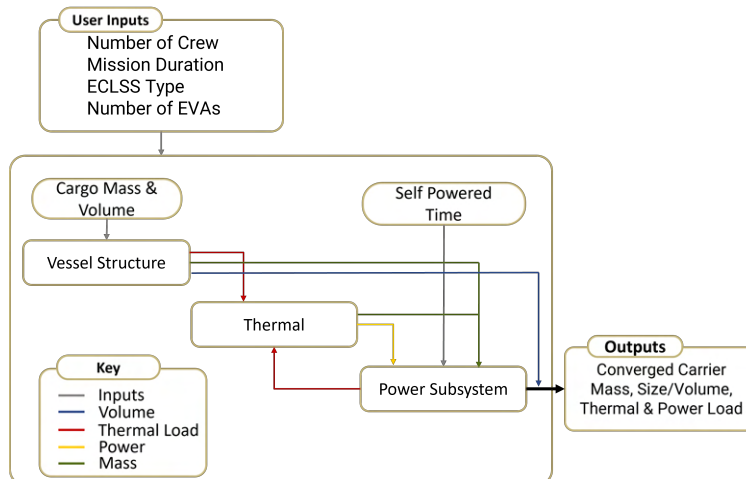


Fig. 5 Simplified N² diagram of Basic Logistic Carrier Module

For a given set of high-level inputs, the corresponding total mass and volume of the resupply consumables and their packaging is computed and fed into the PV model. Furthermore, logistics carriers delivered to the lunar surface via lunar landers need to be transported from the landing site to the habitation module (SH) (large carriers), which is approximately 3.8 km [24] as shown in Fig. 6, or to the pressurized rover (small carriers), which is usually near the SH as well. During transportation, the carrier would most likely rely on its own power to maintain its internal environmental conditions. Additionally, there is the time required for the carrier to dock with the SH or PR once it has reached its destination. The time the carrier needs to rely on its power during these operations is directly fed into the power system.



Fig. 6 Lunar Landing Locations & Approximate End-Use Locations [24]

1. Pressurized Vessel Structure

The PV structure provides structural support, pressurization, and shielding for the resupply cargo from harsh external environmental conditions such as lunar regolith and solar radiation. The model adopts similar assumptions to those made by Cardenas et al. [12], utilizing a monocoque design with a defeatured vessel and circular cross-section for the pressure vessel, as depicted in Fig. 7. This simplification reduces the complexity of the model while maintaining essential details about the hull design. Note that the figure does not illustrate the thickness of the PV structure, although it is accounted for in the model.

The model is parametric, allowing adjustments to the width and height of the internal walkway through which astronauts enter and move within the module. Additional structural elements, such as the number of saddles and the curvature of the beam structure supporting the vessel, can also be adjusted. Once the internal walkway dimensions are set to comfortably accommodate astronauts, the carrier is sized to maximize cargo capacity in the remaining space, based on the logistics module described in [25]. The sections highlighted in light green in Fig.7 indicate the cargo storage areas. As shown, cargo is stored on the sides and back of the carrier module, while the middle section serves as a walkway for astronauts. The radius (R), determined using Eq. 1, represents the minimum internal radius needed to allow astronaut access to the carrier module.

$$R = \sqrt{\left(\frac{h_{\text{int}}}{2}\right)^2 + \left(\frac{w_{\text{int}}}{2}\right)^2} \quad (1)$$

The volumetric constraint for sizing the carrier, see Eq. 2, is derived from the total volume of the resupply cargo and its packaging, along with the volume required to store the batteries inside the carrier. Subsequently, using the cross-sectional area of the cargo storage section of the carrier module, determined using Eq. 3, the lengths of the internal walkway and the PV structure can be calculated, as shown in Eqs. 4 and 5, respectively.

$$V = A_{\text{cs}}L + \pi R^2 \left(R - \frac{w_{\text{int}}}{2}\right) \quad (2)$$

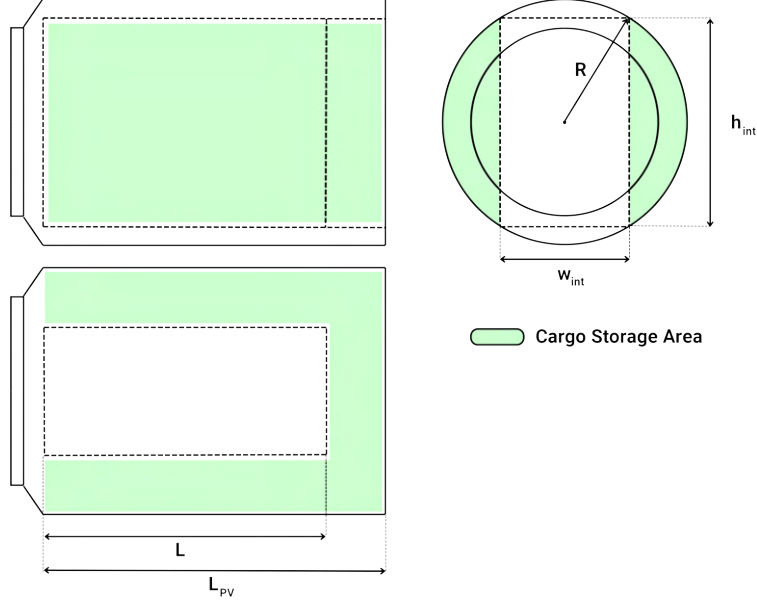


Fig. 7 First Angle View 2D Representation of a Logistic Carrier

$$A_{cs} = \pi R^2 - h_{int} w_{int} - R^2 \left[2 \tan^{-1} \left(\frac{w_{int}}{h_{int}} \right) - \sin \left(2 \tan^{-1} \left(\frac{w_{int}}{h_{int}} \right) \right) \right] \quad (3)$$

$$L = \left[V - \pi R^2 \left(R - \frac{w_{int}}{2} \right) \right] / A_{cs} \quad (4)$$

$$L_{PV} = L + \left(R - \frac{w_{int}}{2} \right) \quad (5)$$

Determining the thickness of the PV structure is another critical parameter in sizing the carrier module. The minimum thickness, see Eqs. 6 and 7, is calculated based on standard atmospheric conditions and assuming the carrier is constructed from aluminum. Both hoop and longitudinal stresses are computed, with the minimum thickness being the greater of the two.

$$t_{min_H} = \frac{PR}{\sigma (SF)} [26] \quad (6)$$

$$t_{min_L} = \frac{PR}{2\sigma (SF)} [26] \quad (7)$$

Finally, to determine the mass and volume of the PV structure, the surface area of the vessel (SA_{PV}) is calculated, see Eq. 8, and the mass and volume are determined by accounting for the minimum thickness of the vessel structure, as shown in Eq. 9 and Eq. 10 respectively.

$$SA_{PV} = 2\pi R L_{PV} + 2\pi R^2 \quad (8)$$

$$m_{PV} = t_{min} SA_{PV} \rho_{Al} \quad (9)$$

$$V_{PV} = \pi (R + 2t_{min})^2 L_{PV} \quad (10)$$

2. Power and Thermal Load

The power and thermal subsystems of the logistic carrier provide the necessary power during self-operation and the required thermal heating/cooling to maintain the internal environment at the desired temperature. These models were adopted from Harding et al. [13]. A lithium-ion battery is used for power storage and is housed within the logistic carrier. For thermal control, a radiator is sized and placed on the external surface of the vessel structure.

The battery sizing model focuses on determining the necessary battery capacity, mass, volume, and heat load for a logistics carrier module. The model accounts for inputs like total power requirements, efficiency, margin, discharge capacity, energy density, volumetric energy density, and operational time. The model ensures that the battery capacity is sufficient to meet the power requirements with added margins for efficiency losses and discharge capacity. It also calculates the mass and volume of the battery based on energy density and volumetric energy density. Additionally, the model estimates the heat load generated by the battery, assuming that the inefficiency results in heat production.

The radiator model is designed to calculate the mass, area, volume, and heat load for a radiator used in a logistics carrier module. The model takes into account various inputs such as illumination (day or night), the pressure vessel's length and radius, its surface area, the maximum temperature, and the heat load from the battery. The model includes functions to calculate the radiator's required area, mass, and volume based on heat dissipation needs, with specific heat flux rejection and radiator mass-volume relationships. This approach ensures that the radiator can effectively manage thermal loads, whether they are from the environment or internal components like batteries.

D. Carrier Output Metrics

To effectively evaluate subsystems, output metrics need to be quantitative, comparable, deterministic from a physics-based perspective, and capable of converging to a final value. In this study, the key metrics for conceptual sizing of the logistics carrier module are carrier mass, volume, power, and thermal load. In this study, the total carrier mass and volume, see Eqs. 11 and 12, are primarily used for analysis and to facilitate trade studies.

$$m_{\text{Carrier}} = m_{\text{PV}} + m_{\text{cargo}} + m_{\text{rack}} + m_{\text{sbeam}} + m_{\text{rad}} + m_{\text{bat}} \quad (11)$$

$$V_{\text{Carrier}} = V_{\text{PV}} \quad (12)$$

E. Design Space Exploration

Once the overall mass and volume of the carrier are computed, the final step is to explore the design space and analyze how the model responds to various mission and design parameters. Each combination of mission parameters from Table 1 can be varied for both small carrier and large carrier logistic module configurations. The design ranges assigned to the continuous variables in the model are shown in Table 4.

Table 4 Design Variables Ranges

Design Variables	Min	Max
Carrier Internal Walkway Height	1.5 m	2.5 m
Carrier Internal Walkway Width	1.0 m	2.0 m
S-beam Arc Angle	120 deg	270 deg
Maximum Temperature	275 K	325 K
Carrier Self Powered Time	6 hrs	48 hrs
Packing Efficiency	0.2 hrs	0.8

A Design of Experiments (DoE) with 10,000 cases was created using a space-filling design with Latin Hypercube Sampling [27], incorporating mission parameters, carrier configurations, and continuous variables to efficiently explore the multi-dimensional parameter space. Each case was then simulated within the MDAO framework, yielding carrier output metrics as response variables. To enable real-time design space exploration and facilitate sensitivity and constraint analysis, surrogate models were developed using neural networks in JMP statistical software. Of the 10,000 cases, 80% were used for training and 20% for validation, and the models were evaluated for accuracy through R^2 , residuals, and Mean Squared Error (MSE)."

V. Case Study: Lunar Resupply Mission

The developed capability was demonstrated through a trade study evaluating the influence of mission parameters and design variables on the sizing of a carrier module. The study assessed key performance outputs for both small and large carrier configurations and examined the feasibility of alternative mission parameters for recurring lunar resupply missions to a pressurized rover. The following subsections will discuss the notional concept of operations and the assumptions used to conduct this study.

A. Concept of Operations

Building on the broader concept of operations (CONOPS) outlined in [14] and further detailed in Section III.B, this study focuses on a specific subset of that architecture as a notional case study to demonstrate the developed capability and assess the feasibility of selected lunar resupply missions. The selected scenario involves two astronauts spending a total of 28 days on the lunar surface, with 14 of those days allocated to a pressurized rover excursion. Accordingly, the objective is to size a carrier module capable of delivering the necessary consumables to sustain both astronauts during the 14-day operation within the pressurized rover.

B. Constraints and Assumptions

One of the main challenges in lunar resupply missions is the transportation and delivery of payloads to the lunar surface [28]. Consequently, when sizing a carrier module intended to resupply a PR, SH, or both, it is important to recognize that in addition to mission parameters and design variables, the mass and dimensional constraints imposed by the delivery vehicle must also be considered.

For this case study, Blue Origin’s Blue Moon Mark 1 lander is selected as the cargo resupply lander for the mission. This uncrewed, medium-class lander is capable of delivering up to 3 metric tons of payload to any location on the lunar surface. Accordingly, the mass and dimensional constraints of the carrier module are defined based on the payload capacity and geometric constraints of this specific lander.

It is also assumed that the surface habitat must be resupplied with sufficient consumables to support two astronauts for the entire duration of their 28-day mission on the lunar surface, including up to 7 extravehicular activities (EVAs). Additional margin is included to account for unforeseen circumstances and enhance crew safety. Under this framework, small carrier modules are sized to deliver consumables for the PR only, supporting two astronauts for a 14-day period and up to 6 EVAs, while large carrier modules are sized to resupply both the SH for the full duration of the mission and the PR for a two-week period.

Lastly, the PR is assumed to operate with an open-loop ECLSS, necessitating continuous resupply of consumables such as oxygen and water. In contrast, the SH is assumed to incorporate a closed-loop ECLSS, capable of recycling key fluids, thereby significantly reducing the volume of recurring consumables required for resupply.

VI. Results

This section presents an analysis of results and key observations using data obtained from the logistics resupply approximation tool, the parametric MDAO framework, and surrogate modeling. Using the use case mission parameters shown in Table 5 as a starting point, the mass breakdown of consumables is first presented. This is followed by a sensitivity analysis to evaluate the variability of the output metrics with respect to the mission and design inputs. Finally, a constraint analysis is conducted to assess the feasibility of point designs and compare small carriers to large carriers for the selected use case.

Table 5 Use case Mission Parameter Inputs

Mission Parameter	Selected Alternative
Number of Crew	2
Mission Duration (days)	14
ECLSS Type (Closure)	Open
Number of EVAs	6

A. Resupply Consumables Mass Breakdown

The logistics resupply approximation tool calculates the consumables needed to sustain a PR with 2 crew members over a 14-day mission. In this scenario, each astronaut can perform up to 6 EVAs. Table 6 provides the results for an "open-loop" ECLSS, where all recycling occurs on the SH, requiring continuous resupply of consumables. In contrast, Table 7 shows the results for a "closed-loop" ECLSS, where water and carbon dioxide are recycled, allowing the PR to regenerate these resources and reduce the amount of consumables needed.

Figures 8 and 9 illustrate the mass breakdown of consumables for "open-loop" and "closed-loop" ECLSS configurations, respectively. It is important to note that fluids and their packaging constitute most of the resupply mass. However, the ability of the PR to recycle some fluids can significantly decrease the required resupply mass and volume. In this study, the "closed-loop" ECLSS configuration results in a 29.15% reduction in the resupply mass for a PR.

Table 6 Open ECLSS Results Summary

Item	Mass (Kg)	Volume (m ³)
Food + CTB	76.84	0.21
Other Consumable Solids + CTB	72.49	0.53
Water + Carrier	191.31	0.64
Oxygen + Carrier	343.57	1.27
Nitrogen + Carrier	75.78	0.32
Spares + CTB	78.49	0.16
Open Total	838.48	3.13

Table 7 Closed ECLSS Results Summary

Item	Mass (Kg)	Volume (m ³)
Food + CTB	76.84	0.21
Other Consumable Solids + CTB	72.49	0.53
Water + Carrier	115.86	0.42
Oxygen + Carrier	173.46	0.64
Nitrogen + Carrier	75.78	0.32
Spares + CTB	79.66	0.11
Closed Total	594.09	2.23

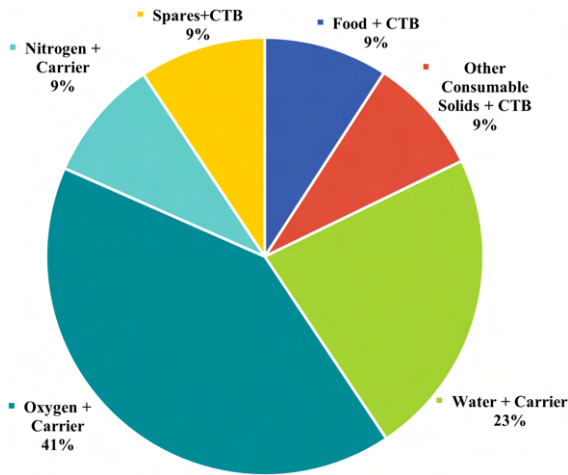


Fig. 8 Open ECLSS Mass Breakdown

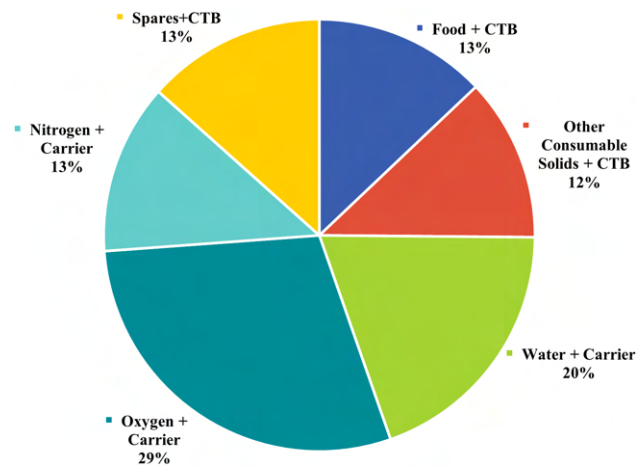


Fig. 9 Closed ECLSS Mass Breakdown

B. Sensitivity Analysis

This section assesses the sensitivity of the model outputs (total carrier mass, volume, and length) to various model inputs (design and mission parameters) using surrogate models. Fig. 10 presents prediction profiler plots generated in JMP statistical software, visualizing these sensitivities. The profiler indicates that the carrier configuration (small or large carrier) significantly influences the carrier size and mass sensitivity.

Figures 11, 12 and 13 present a ranked sensitivity analysis that quantifies the impact of individual input variables on the output metrics, with all other variables held constant. Although mission parameters are the main drivers of carrier mass sensitivity, design parameters, such as packing efficiency and height and width of the internal walkway, play a more significant role in influencing the carrier's geometric constraints.

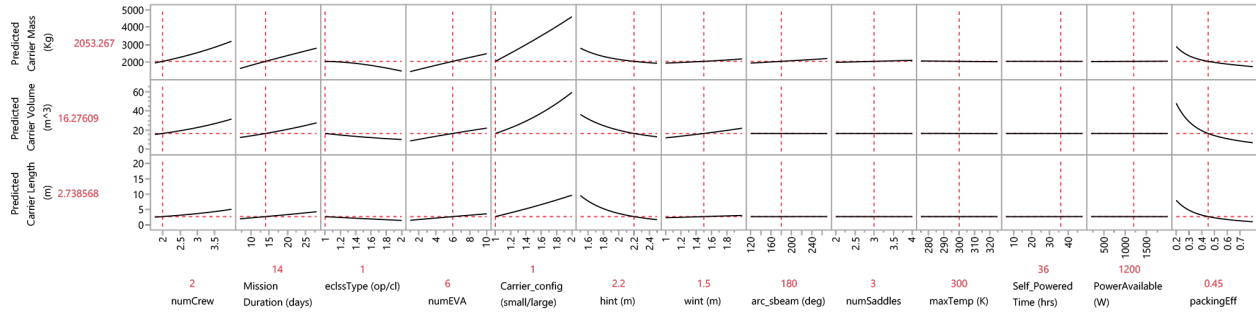


Fig. 10 Sensitivity of Output Metrics to Inputs

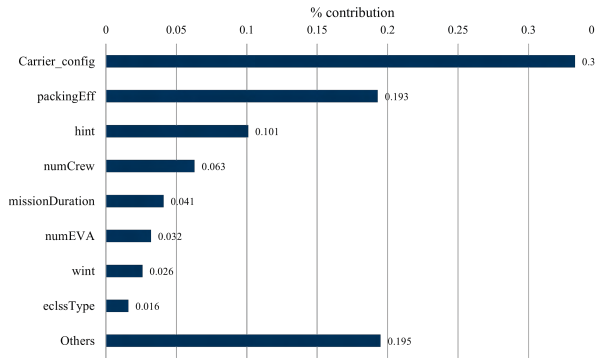


Fig. 11 Carrier Mass Sensitivity

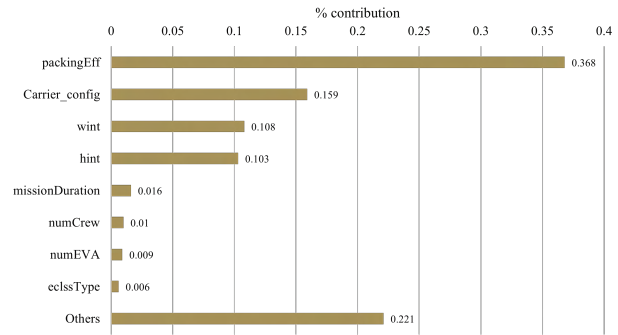


Fig. 12 Carrier Volume Sensitivity

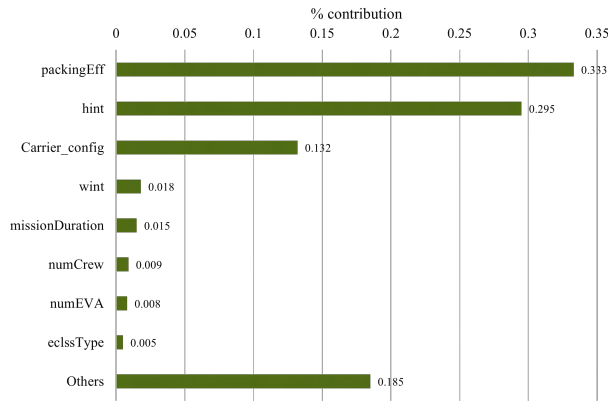


Fig. 13 Carrier Length Sensitivity

C. Constraint Analysis

Using the surrogate model and information from the sensitivity analysis, this section conducts a constraint analysis to evaluate the feasibility of point designs for the presented use case. The range of values for the mission and design parameters are based on Tables 1 and 4. The constraints for carrier mass, volume, and length are derived from the lunar cargo lander that delivers the carriers. The mass and volume constraints are the maximum payload capacity and cargo bay volumetric size of the lander, while the length constraint is the maximum carrier length that the lander can accommodate. For this study, Blue Origin’s Blue Moon MK1 lander is used.

Figure 14 shows the design space for a small carrier sized according to the defined mission parameters. The figure indicates that there is a point design that meets the mass, volume, and length constraints of the lander. According to NASA, the estimated mass of a resupply logistics module for the mission parameters used in this study is approximately 2000 kg [16] [24]. The mass of the carrier obtained for this point design, which serves as the baseline for this study, is

2053.27 kg, a difference of less than 3% from NASA’s estimation. This is within acceptable bounds for a conceptual sizing of space vehicles and hence verifies the model’s accuracy.

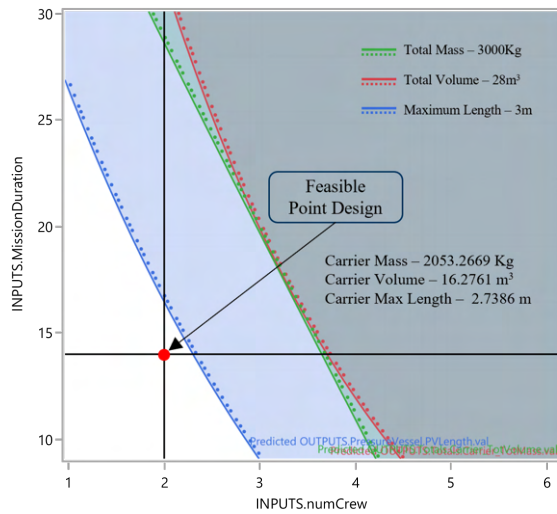


Fig. 14 Small Carrier Baseline Design Space

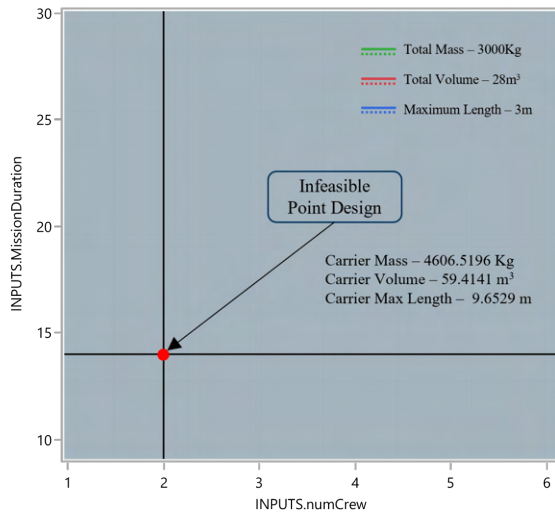


Fig. 15 Large Carrier Baseline Design Space

When examining the design space for large carriers, as illustrated in Fig.15, it becomes evident that the carrier module exceeds the size and weight constraints set by the MK1 lander. Consequently, no feasible point design exists for the given mission and design parameters. One approach to open the design space is to relax these constraints, which would necessitate the use of a larger cargo lander for the mission. NASA’s recent white paper on Lunar Surface Cargo from its Moon to Mars Architecture supports this need [16]. Appendix B presents NASA’s planned lander capabilities versus surface cargo demand, indicating a requirement for a lander that can accommodate resupply cargo ranging from 500 kg to 12,000 kg. While larger landers, such as SpaceX’s Starship cargo variant or Blue Origin’s MK2, can handle significantly larger payloads, they are not specifically designed for the periodic delivery of resupply logistics carriers unless these modules are included as secondary payloads alongside larger primary payloads.

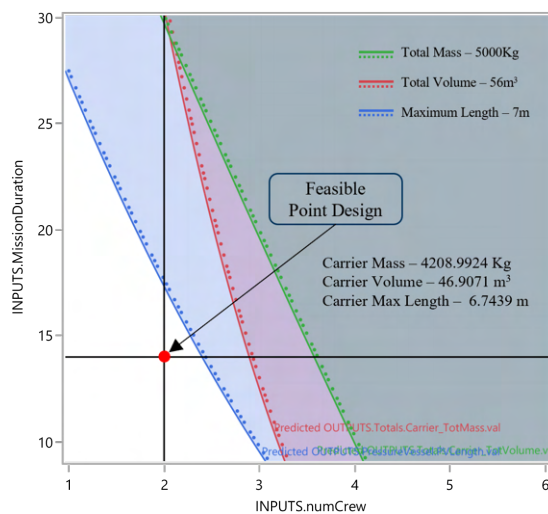


Fig. 16 Large Carrier Alternative Design Space

In addition to the increased mass, another important observation associated with large carrier configurations is the change in geometry. As more cargo is packaged into a single carrier, the overall length of the module increases significantly. To address this, adjustments to specific design variables are required. Sensitivity analysis reveals that the carrier geometry is most influenced by two design parameters: packaging efficiency and internal walkway height. By

implementing modest changes, such as increasing the packaging efficiency by 5% and slightly increasing the internal walkway height by just under 10%, the carrier length can be reduced sufficiently to satisfy the geometric constraints of a future-class lander.

Should such a lander become available, constraints would be relaxed, thereby expanding the design space. Fig. 16 depicts a notional design space for a large carrier with a feasible point design, contingent on the availability of a resupply cargo lander that meets the payload requirements of a large carrier.

VII. Conclusion

This study presented a comprehensive approach for sizing and evaluating the feasibility of logistics carrier designs to support lunar resupply missions. Using a parametric MDAO framework and a custom Logistics Resupply Approximation Tool (LRAT), the analysis explored how mission and design parameters affect the mass, volume, and geometry of carrier modules intended to resupply a pressurized rover (PR) and surface habitat (SH).

Sensitivity and constraint analyses showed that small logistics carriers, designed specifically for PR resupply, are feasible within the payload limitations of Blue Origin's Blue Moon MK1 lander. These carriers meet the lander's mass, volume, and length constraints, making them suitable for current lunar mission concepts. In contrast, large carriers, which are designed to resupply both the PR and SH, exceed the MK1's geometric and mass limitations, and no feasible point designs were found under the existing constraints.

However, the study also showed that by adjusting key design variables, such as increasing the packing efficiency and internal walkway height, the length of the large carrier can be reduced to fit within the expected constraints of a future-class lander. These findings underscore the need for the development of a new class of lunar cargo lander with greater mass and volumetric capacity specifically tailored for recurring resupply missions. This aligns with NASA's lunar surface cargo studies, which highlight a significant capability gap between existing small landers and large human-rated landers.

In summary, while small carriers are a practical solution under existing constraints, large carriers present a promising option for future missions, contingent on the development of more capable lunar cargo landers. This study uses sensitivity analysis and constraint analysis through surrogate modeling to provide quantitative basis for decision making. It offers a structured approach to evaluate the impact of mission and design parameters and supports early-phase trade studies that inform strategic planning for future lunar resupply architectures.

Appendix

A. Data Flow N2 Diagram from OpenMDAO

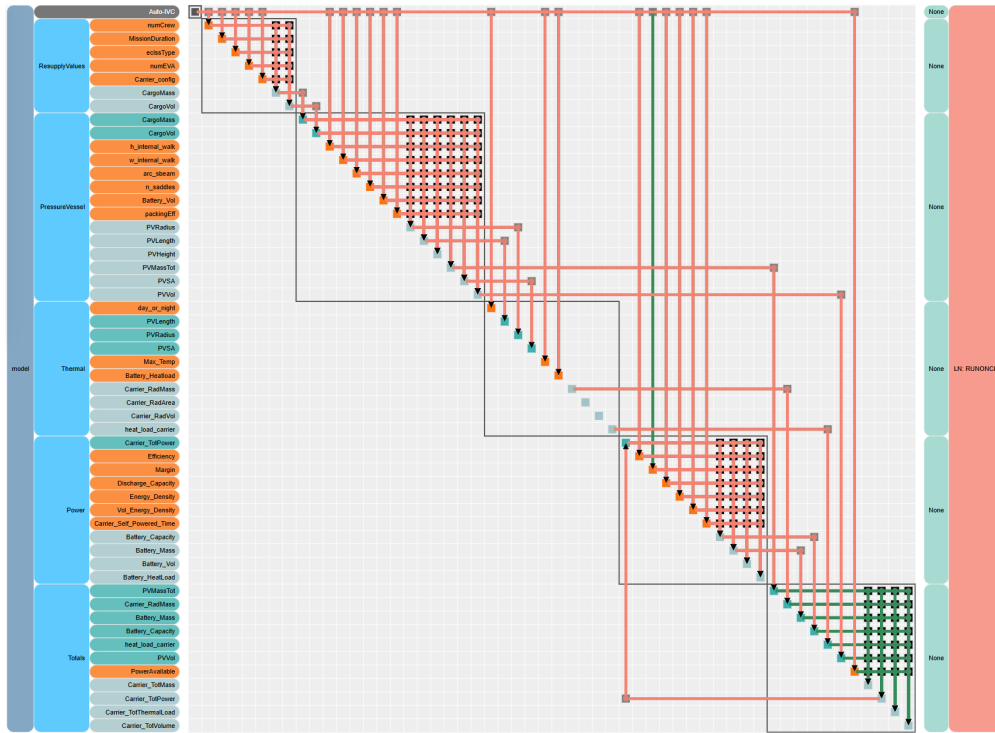


Fig. 17 Appendix A: Data Flow N2 Diagram from OpenMDAO

B. NASA resupply cargo needs and cargo lander demands [16]

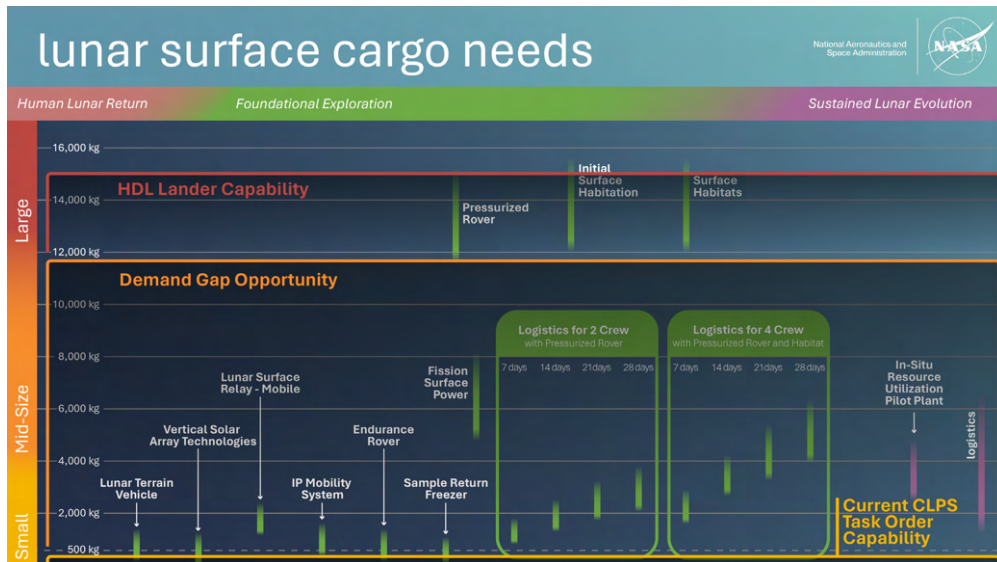


Fig. 18 Appendix B: NASA resupply cargo needs and cargo lander demands

Acknowledgments

The authors would like to thank Dr. Bill O’Neill for his guidance in defining the problem and Fernando A. Morales for reviewing and providing insightful feedbacks throughout the study.

References

- [1] Merancy, N. F., “Moon to Mars Architecture Executive Overview,” , January 2024. URL <https://ntrs.nasa.gov/citations/20240000449>, nTRS Author Affiliations: Johnson Space Center; NTRS Document ID: 20240000449; NTRS Research Center: Headquarters (HQ).
- [2] Goodliff, K. E., Merancy, N. F., Bhakta, S. S., Rucker, M. A., Chai, P. R.-P., Ashurst, T. E., Troutman, P. A., and Stromgren, C., “Exploration Systems Development Mission Directorate (ESDMD) Moon-to-Mars Architecture Definition Document,” , April 2023. URL <https://ntrs.nasa.gov/citations/20230002706>.
- [3] Stromgren, W., and States), N. A. A. A. M. A. U., “Lunar Logistics Drivers and Needs,” , February 2024. URL <https://ntrs.nasa.gov/citations/20230016304>, NTRS Document ID: 20230016304, NTRS Research Center: Headquarters (HQ).
- [4] Goodliff, K. E., Stromgren, C., Dickert, Z., Ewert, M. K., Hill, J., and Moore, C., “Logistics Needs for Future Human Exploration Beyond Low Earth Orbit,” *AIAA SPACE and Astronautics Forum and Exposition*, AIAA SPACE Forum, American Institute of Aeronautics and Astronautics, 2017. <https://doi.org/10.2514/6.2017-5122>.
- [5] Lynch, C., Goodliff, K. E., Stromgren, C., Vega, J., and Ewert, M. K., “Logistics Rates and Assumptions for Future Human Spaceflight Missions Beyond LEO,” *ASCEND 2023*, ASCEND, American Institute of Aeronautics and Astronautics, 2023. <https://doi.org/10.2514/6.2023-4617>.
- [6] Lioy, S., Provera, R., and Ciampolini, A., “International Space Station Logistics Through the Multi-Purpose Logistics Module,” *AIAA International Air and Space Symposium and Exposition: The Next 100 Years*, International Air and Space Symposium (Evolution of Flight), American Institute of Aeronautics and Astronautics, 2003. <https://doi.org/10.2514/6.2003-2702>.
- [7] Congiardo, J., Buckles, B., Felt, A., Lasater, J., Nufer, B., Krenn, A., Lewis, M., McCleskey, C., Perotti, J., Tamasy, G., Thompson, J., Bielski, P., Li, Z. Q., Whittington, P., Blake, C., Dodd, K., Hoffman, S., Phillips-Hungerford, T., Baysinger, M., Rogan, J., and Chappell, M. B., “Assessment of a Surface Water Transportation System Concept for ISRU Operations on Mars,” *AIAA SCITECH 2024 Forum*, AIAA SciTech Forum, American Institute of Aeronautics and Astronautics, 2024. <https://doi.org/10.2514/6.2024-2541>.
- [8] Congiardo, J., Lewis, M. E., McCleskey, C. M., Reeves, C. T., Swanger, A., Tamasy, G., Bielski, P., Blake, C., Dodd, K., Hoffman, S., Li, Z. Q., Phillips-Hungerford, T., Whittington, P. A., Chappell, M. B., Choate, A. J., and Owens, J. E., “Assessment of a Mars Surface Cryogenic Transportation System,” *AIAA SCITECH 2025 Forum*, AIAA SciTech Forum, American Institute of Aeronautics and Astronautics, 2025. <https://doi.org/10.2514/6.2025-0513>.
- [9] Harrison, D. A., Ambrose, R., Bluethmann, B., and Junkin, L., “Next Generation Rover for Lunar Exploration,” *2008 IEEE Aerospace Conference*, 2008, pp. 1–14. <https://doi.org/10.1109/AERO.2008.4526234>, ISSN: 1095-323X.
- [10] Trent, D. J., Edwards, S. J., and Chappell, M. B., “Design of a Family of Mars Chemical Transportation Elements,” 2024. URL <https://ntrs.nasa.gov/citations/20230017880>, NTRS Author Affiliations: Marshall Space Flight Center NTRS Document ID: 20230017880 NTRS Research Center: Marshall Space Flight Center (MSFC).
- [11] Bhardwaj, M., Bulsara, V., Kokan, D., Shariff, S., Svarverud, E., and Wirz, R., “Design of a pressurized lunar rover,” , April 2024. URL <https://ntrs.nasa.gov/citations/19930008827>, NTRS Author Affiliations: Virginia Polytechnic Inst. and State Univ. NTRS Document ID: 19930008827 NTRS Research Center: Legacy CDMS (CDMS).
- [12] Cardenas Melgar, A., Puri, N., Robertson, B. E., and Mavris, D. N., “Creation of a Structural Model to Facilitate an OpenMDAO-Based Lunar Rover Parametric Sizing Tool,” *AIAA SCITECH 2024 Forum*, AIAA SciTech Forum, American Institute of Aeronautics and Astronautics, 2024. <https://doi.org/10.2514/6.2024-0768>.
- [13] Harding, C., Peak, V., Robertson, B. E., and Mavris, D. N., “Power and Thermal System Modeling for a Pressurized Lunar Rover,” *AIAA SCITECH 2024 Forum*, AIAA SciTech Forum, American Institute of Aeronautics and Astronautics, 2024. <https://doi.org/10.2514/6.2024-2372>.
- [14] Kessler, P., Prater, T., Nickens, T., and Harris, D., “Artemis Deep Space Habitation: Enabling a Sustained Human Presence on the Moon and Beyond,” *2022 IEEE Aerospace Conference (AERO)*, IEEE, 2022, pp. 01–12. <https://doi.org/10.1109/AERO53065.2022.9843393>.

- [15] LSIC, “LunA-10 LSIC Performer Binder,” , April 2024. URL <https://lsic.jhuapl.edu/uploadedDocs/meetings/docs/2441-DISTRO%20A%20LunA-10%20LSIC%20Performer%20Binder.pdf>, presented at the Lunar Surface Innovation Consortium (LSIC) Meeting.
- [16] NASA, “Lunar Surface Cargo: Enabling Sustained Lunar Exploration,” , June 2024. URL <https://www.nasa.gov/wp-content/uploads/2024/06/acr24-lunar-surface-cargo.pdf?emrc=660c66>.
- [17] Howard, R. L., “Human Factors Considerations for Pressurized Crew Transfer Between Ascent or Lander Spacecraft and Surface Assets,” *ASCEND 2021*, ASCEND, American Institute of Aeronautics and Astronautics, 2021. <https://doi.org/10.2514/6.2021-4020>.
- [18] Ewert, M. K., Chen, T. T., and Powell, C. D., “Life Support Baseline Values and Assumptions Document,” , February 2022. URL <https://ntrs.nasa.gov/citations/20210024855>, NTRS Author Affiliations: Johnson Space Center, Jacobs (United States) NTRS Document ID: 20210024855 NTRS Research Center: Johnson Space Center (JSC).
- [19] “Human Integration Design Handbook (HIDH),” Tech. Rep. SP-2010-3407 Rev 1, NASA, Washington, D.C., 2014. URL https://www.nasa.gov/wp-content/uploads/2015/03/human_integration_design_handbook_revision_1.pdf.
- [20] Akin, D., and Bowden, M., “A Small Pressurized Rover Concept for Extended Lunar and Mars Exploration,” *Space 2005*, AIAA SPACE Forum, American Institute of Aeronautics and Astronautics, 2005. <https://doi.org/10.2514/6.2005-6737>.
- [21] Burke, C. J., and Howard, R. L., “Internal Layout Assessment of a Lunar Surface Habitat,” *ASCEND 2022*, ASCEND, American Institute of Aeronautics and Astronautics, 2022. <https://doi.org/10.2514/6.2022-4266>.
- [22] Bagdigian, R., and Stambaugh, I., “An Environmental Control and Life Support System Concept for a Pressurized Lunar Rover,” *40th International Conference on Environmental Systems*, International Conference on Environmental Systems (ICES), American Institute of Aeronautics and Astronautics, 2010. <https://doi.org/10.2514/6.2010-6256>.
- [23] Gray, J., Moore, K., and Naylor, B., “OpenMDAO: An Open Source Framework for Multidisciplinary Analysis and Optimization,” *13th AIAA/ISSMO Multidisciplinary Analysis Optimization Conference*, American Institute of Aeronautics and Astronautics, 2010. <https://doi.org/10.2514/6.2010-9101>.
- [24] NASA, “Lunar Mobility Drivers and Needs,” Tech. rep., NASA, 2024. URL <https://www.nasa.gov/wp-content/uploads/2024/06/acr24-lunar-mobility-drivers-and-needs.pdf?emrc=b2dafa>, accessed: 2024-07-30.
- [25] Smitherman, D. V., Canerday, S., Perry, J., and Howard, D., “Concepts for Phased Development of a Lunar Surface Base,” *ASCEND 2020*, ASCEND, American Institute of Aeronautics and Astronautics, 2020. <https://doi.org/10.2514/6.2020-4051>.
- [26] Moss, D. R., *Pressure Vessel Design Manual*, Gulf Professional Publishing, 200 Wheeler Road, Burlington, MA 01803, USA, 2004.
- [27] Lu, L., Anderson-Cook, C., Martin, M., and Ahmed, T., “Practical choices for space-filling designs,” Vol. 38, 2021. <https://doi.org/10.1002/qre.2884>.
- [28] Cirillo, W., Earle, K., Goodliff, K., Reeves, j. D., Andrashko, M., Merrill, R. G., and Stromgren, C., “Analysis of Logistics in Support of a Human Lunar Outpost,” 2008. URL <https://ntrs.nasa.gov/citations/20080042297>.